國 立 交 通 大 學

電機學院　電信學程

碩 士 論 文

低溫共燒陶瓷技術之非平衡至平衡及電容抽頭分接式交

連濾波器暨射頻平衡輸入至平衡輸出帶通濾波器研究

Research on Unbalanced to Balanced Band-pass Filter with
Tapped Capacitor for Selectivity Improvement Using LTCC
and Balanced Input-Output Band-pass Filter

研 究 生：吳能炎　　　　　　(Nen-Yen Wu)

指導教授：鍾世忠 教授　　　(Dr. Shyh-Jong Chung)

中 華 民 國 九十七年 六 月

低溫共燒陶瓷技術之非平衡至平衡及電容抽頭分接式交連濾波器暨射頻平衡輸入至平衡輸出帶通濾波器研究

Research on Unbalanced to Balanced Band-pass Filter with Tapped Capacitor for Selectivity Improvement Using LTCC and Balanced Input-Output Band-pass Filter

研 究 生：吳能炎　　　　　Student: Nen-Yen Wu

指導教授：鍾世忠　　　　　Advisor: Dr. Shyh-Jong Chung

國立交通大學

電機學院　電信學程

碩士論文

A Thesis

Submitted to College of Electrical and Computer Engineering

National Chiao Tung University

in partial Fulfillment of the Requirements

for the Degree of

Master of Science

In

Communication Engineering

June 2008

HsinChu, Taiwan, Republic of China

中 華 民 國 九十七 年 六 月

低溫共燒陶瓷技術之非平衡至平衡及電容抽頭分接式交連濾波器暨射頻平衡輸入至平衡輸出帶通濾波器研究

研 究 生：吳能炎　　　　　　　指導教授：鍾世忠 教授

國立交通大學　電機學院　電信學程碩士班

中文摘要

本篇論文前段旨在已知的 Marchan Balun 結構中，利用輸入傳輸線的開路尾端(open end)直接接地，並於輸入端加上一對地電容使其產生共振腔而形成一帶通濾波器。此特性更別於以往傳統 Marchan Balun，特別在輸出的平衡端點上跨接一電容器，使其輸出傳輸線經由地的連接串聯形成一段連續電感，並產生另一共振腔而形成一帶通濾波。因此這樣的兩個共振腔經由 Marchan Balun 的交連耦合特性就可以形成一個有帶通濾波器特性的 Balun。 由於為了提升其選擇性，使用電容抽頭 Tapped-Capacitor 的方試進行耦合交連，用升阻的方式來提升並聯共振 Q 值(circuit Q)，並且提升通帶的頻率響應特性且利用低溫共燒陶瓷多層架構的技術，來完成此一平衡式帶通濾波器的設計。平衡式射頻輸入至平衡式射頻輸出帶通濾波器由於中心頻率設計於 2.4GHz，所以此帶通濾波器適用於藍牙或無線區域網路(IEEE 802.11b/g)之應用中。

在本篇論文的後段，則是利用已經知悉方式在 Marchan Balun 輸出的平衡端點上跨接一電容器和使其輸出傳輸線經由地的連接串聯，形成一段連續電感並產生一並聯共振，此外在輸入端以背靠背的方式建構另

一平衡輸入端，經由兩個共振腔的交連耦合特性就可以形成一平衡式射頻輸入至平衡式射頻輸出帶通濾波器，並利用 R/T Duroid/5880 substrate 及 high-Q discrete 陶瓷電容來完成實驗印證。此一帶通濾波器可用於提升射頻信號能力，此一設計用於接續平衡射頻輸入如 Dipole Antenna。由於 2.4GHz 的設計所以此帶通濾波器亦適用於藍牙或無線區域網路 (IEEE 802.11b/g)之應用中。

Research on Unbalanced to Balanced Band-pass Filter with Tapped Capacitor for Selectivity Improvement Using LTCC and Balanced Input-Output Band-pass Filter

Student:Nen-Yen Wu   Advisor: Dr. Shyh-Jong Chung

Degree Program of Electrical and Computer Engineering
National Chiao Tung University

Abstract

This study proposes an unbalanced to balanced band-pass filter and a balanced input-output band-pass filter. Firstly, an unbalanced to balanced band-pass filter which is composed from a Marchand balun circuitry using Low Temperature Co-fired Ceramic (LTCC) technology is proposed and designed. Based on the Marchand balun, this work uses a shunt capacitor connecting the input port to ground, and then lets the open end of the input transmission line be short to ground, thus can derive a resonator. Besides, a capacitor is connected between the two balanced output ports of the Marchand balun, and remaining the other end of each output transmission line connected to ground. Therefore, it can form another resonator. For improving the performance of selectivity, tapped-C is used to enhance the circuit Q of the resonator and to couple the signal to the next stage. The proposed unbalance to balance band-pass filter which has low insertion loss at pass band and good attenuation at suppression area can be applied in Bluetooth or IEEE 802.11b/g WLAN (Wireless Local Area Network).

Secondly, a balanced to balanced band-pass filter is proposed. Also based on the Marchand balun mentioned above, a capacitor is connected between the two balanced output ports, and thus forms a parallel-LC resonator by co-operating the grounded

transmission line. After duplicating the same balanced ports with back-to-back structure, a balanced to balanced band-pass filter is derived.

In order to verify the circuit simulation, we used low loss R/T Duroid/5880 substrate and high-Q discrete ceramic capacitors to implement the experiment circuit. The proposed balanced to balanced band-pass filter can also be applied in Bluetooth or IEEE 802.11b/g WLAN (Wireless Local Area Network).

誌謝

在交大電信研究這幾年的時間，由於需一面工作並需前往海外工廠及照顧家庭，僅能利用片段時間來修碩士學位，慶得鍾世忠教授的體諒，讓我在微波及射頻的知識收穫甚多，這真的要很感謝鍾世忠教授的細心指導。這幾年來跟著老師做研究，讓我在工作上更能得心順手而得到了擢升的機會及更有研究的精神，更多的是在做人處事上的態度與方法，這些都讓我終身受益。同時要感謝實驗室所有的成員：珮華、阿信、嘉言、淑君、有你們的協助。

另外，我也要感謝我的眾多長官同事廠商同學與朋友們：文弘、建成、生明、林暉、柏湖、昆賜、嘉言、鈞富、小麗、林經理 等的協助及提攜，讓我這幾年的日子過得充實及美好，謝謝你們！

最後要感謝我的家人慧玉、予捷、小胖，這些年來的鼓勵與支持，讓我可以在工作及學業上有更上一層的機會，如今你們的付出，讓我可以順利的完成研究所的學業，感謝你們

Contents

List of Figures

Chapter 1   Introduction

Balanced circuits are important in building a modern communication system due to better gain and second-order linearity, superior spurious response performance, and noise immunity. Analog signals processed by a communication system are degraded by two different types of noises, namely, the environmental noise and device electronic noise. The former refers to the random disturbances that a circuit experiences through the dc power supply, ground lines, or substrate coupling. The latter includes the thermal noise, shot noise, and flicker noise, which comes from the internal active device [1]. Most of RF low-noise amplifier or balanced mixers which have the differential signal format are often used in Silicon CMOS circuits for their excellent rejection of common-mode substrate noise. It still needs single-ended components, such as the antenna and the filter, in the RF front-end module.

An unbalanced to balanced component, such as balun, is thus necessary to be put between the single-ended RF front-end module and the balanced chipset. The balun is a passive electronic device that converts balanced transmission signal into an unbalanced signal and vice versa. In a balun, one pair of terminals is balanced, that is, the currents are equal in magnitude and opposite in phase. The other pair of terminals is unbalanced; one side is connected to electrical ground and the other carries signal [2]. Due to the selectivity of RF devices are based on out-of-band suppression, therefore, a band-pass filter is often used to cascade the balun to reach such a performance. There are many literatures investigating the configurations and the performance of the balun and band-pass filter on [3]-[9],

The thesis proposes a differential band-pass filter which is composed from a Marchand balun circuitry, the resonated capacitors, and a balanced to balanced band-pass filter. The Marchand balun is realized with two sets of folded broadside-coupled lines to fully utilize the LTCC multilayer advantage. The circuit is simulated by 3D EM simulator [14] to optimize the band-pass performance. The filters has been designed by using circuit simulation as well as full-wave electromagnetic (EM) simulation tool. The measured results agree very well with the simulated results. This shows great application potentials of the proposed differential LTCC band-pass filter in wireless single-chip RF transceivers. Besides, the structure of balanced to balanced filter should be connected to a dipole antenna to RF transceivers also. This thesis consists of four chapters. Chapter 1 gives the brief introduction of balanced band-pass filter. In chapter 2, the configuration of the Marchand balun with advanced poles of resonator suitable for IEEE 802.11b/g WLAN is proposed. The theory analysis, 3-D LTCC layouts, EM simulation and measurement results are also presented in chapter 2. In chapter 3, a balanced to balanced band-pass filter is proposed and designed. The design concept is based on the previous description of balanced filter. Additionally, the circuit simulation and measurements are also presented in this chapter. At last, conclusions are followed in chapter 4.

Chapter 2   Unbalanced to Balanced Band-pass Filter

The conventional band-pass filter is usually in a single-ended structure, which requires an additional balun to connect to the differential RF low-noise amplifier or balanced mixers. The differential signal format is often used in modern Silicon CMOS circuits for their excellent rejection of common-mode substrate noise. In this differential band-pass filter design, the balun is incorporated into the band-pass filter circuitry such that a miniaturized fully-integrated LTCC band-pass filter can be used directly between the antenna and the single-chip differential CMOS RF transceiver. A good band-pass filter has low pass-band insertion loss and provides large suppression in the rejection area including the image signal and in-band signal harmonics. High suppression in rejection area can be provided by generating transmission zeros at the rejection frequencies or good sharpness performance in skirt area.

This chapter describes the theory and design with the Marchand balun, which uses a shunt capacitor connecting the input port to ground, and then lets the open end of the input transmission line be short to ground, thus can derive a resonator. Besides, a capacitor is connected between the two balanced output ports of the Marchand balun, and remaining the other end of each output transmission line connected to ground. Therefore, it can form another resonator. The section 2.1 describes the theory of skill tapped-C for enhancing the circuit Q of the resonator to improve the selectivity performance of the band-pass filter and to couple the signal to the next stage. Furthermore, the theory analysis, 3-D LTCC layouts, EM simulation and measurement results are also presented in Chapter 2.

2.1 Theory and Design

The schematic of the conventional balun is shown at Fig.2.1, the balun represents the common Marchand transmission line balun [12], let's investigate behavior of the balun's characteristics in wider frequency band. Considering to method described in [11], the balun's amplitude characteristic is periodical and one period consists of transmission band and notches. As shown in Fig.2.2, the balun has a simple harmonic rejection due to a notch at 6.5GHz.
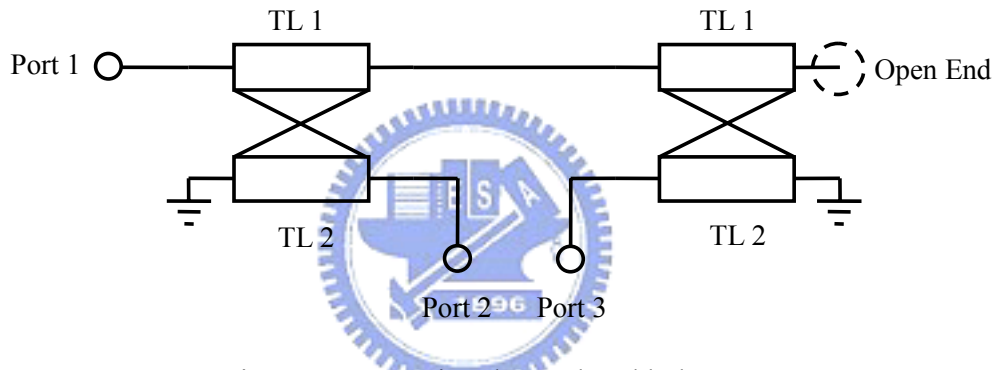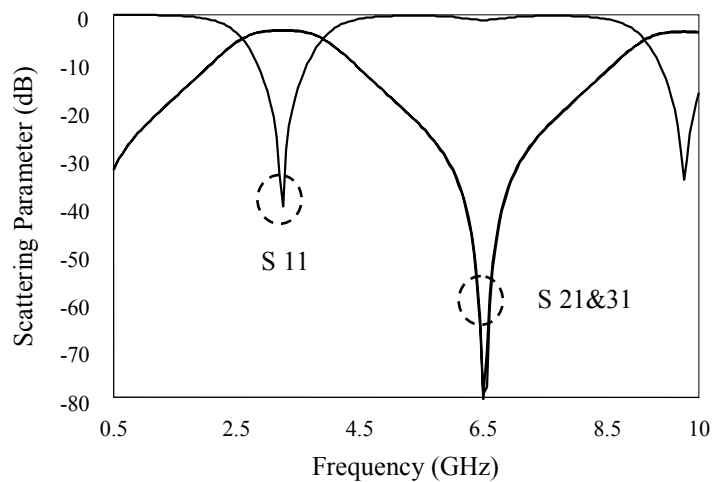

Fig. 2.1 Conventional Marchand balun

Fig. 2.2 Characteristics of the Marchand balun using ideal elements, also illustrates the result of Fig.2.1

The schema of the unbalanced to balanced band-pass filter is shown in Fig. 2.3, it is represented as modification of the common Marchand transmission line balun [10]-[12]. Compact designs to miniaturize the balun were reported in literature [10]. TL_1, which has the short end of the transmission line, has Z_X – complex impedance that used for improving of the circuit's matching. The prototype of the proposed schema appears as the result of the balun's miniaturization. Capacitors, CT_1, CT_2 and C_2 are used for contraction of the transmission line (TL). In Fig. 2.3, in the upper network of the schema of the Marchand balun, CT_1 is cascaded to CT_2 and the strip-line section TL_1 is connected to ground to form a resonator with the lower network C_2 between the balanced output portions of the Marchand balun. Besides, the end of the two transmission lines of output ports is connected to ground. Therefore, that will generate another resonator. The two resonators can generate two poles, supporting the filter's pass-band. The equivalent circuit is shown in Fig.2.4. It is the filter with coupled resonators that provides impedance transformation and balanced outputs. It should be taken into account that changing the line's length during optimization causes the frequency offset of the center working frequency and the change of the bandwidth. To improve the selectivity performance of the balanced band-pass filter, we use the skill of tapped-C to improve the circuit loaded Q of the resonator and to couple the signal to the next stage.
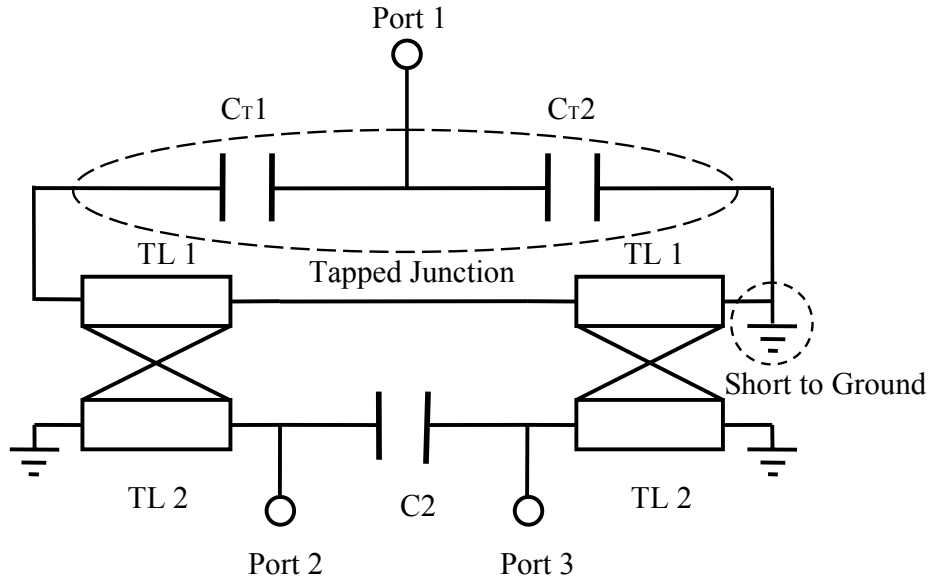
Fig. 2.3 Schema of the balanced filter with tapped capacitors and one end of the input
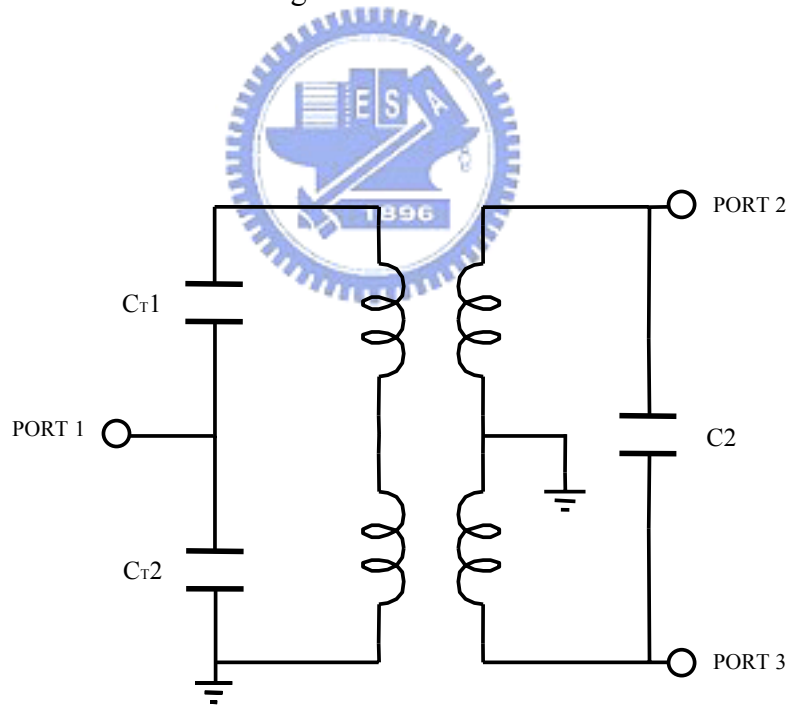transmission line connected to ground

Fig. 2.4 The equivalent lumped circuit

Fig. 2.5 shows the simulation result of Fig. 2.3. It is calculated with the circuit simulator *Microwave Office* [13], both results of circuit simulation are shown and compared in Fig. 2.5. The solid line indicates result of circuit simulation with tapped-C for selectivity improvement, and the dashed line represents circuit simulation without tapped-C. From the circuit-simulated scattering parameters shown in Fig 2.5, it agrees with the expectation of the previous discussion of the tapped capacitor for which impedance transformation will reach narrow-bandwidth and better selectivity in out-of-band of high skirt side. It can be observed from S_{21} and S_{31} that the filter with tapped-C is 10dB sharper than the one without tapped-C.
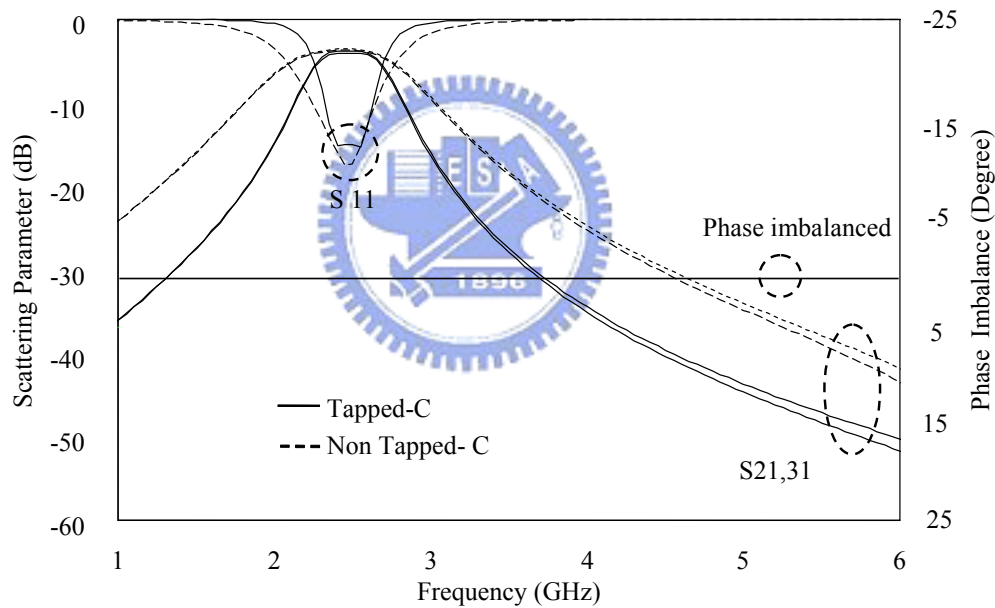
Fig. 2.5 Selectivity comparison between filters with and without tapped capacitor

The selectivity of the band-pass filter can be solved graphically. Fig. 2.6 depicts the different load impedance shunt with parallel-LC resonator. The simulation illustrates that the high impedance will reach the better sharpness in skirt area of band-pass filter. The simulated results shown in Fig. 2.6 are calculated with the circuit simulator *Microwave Office* [13].
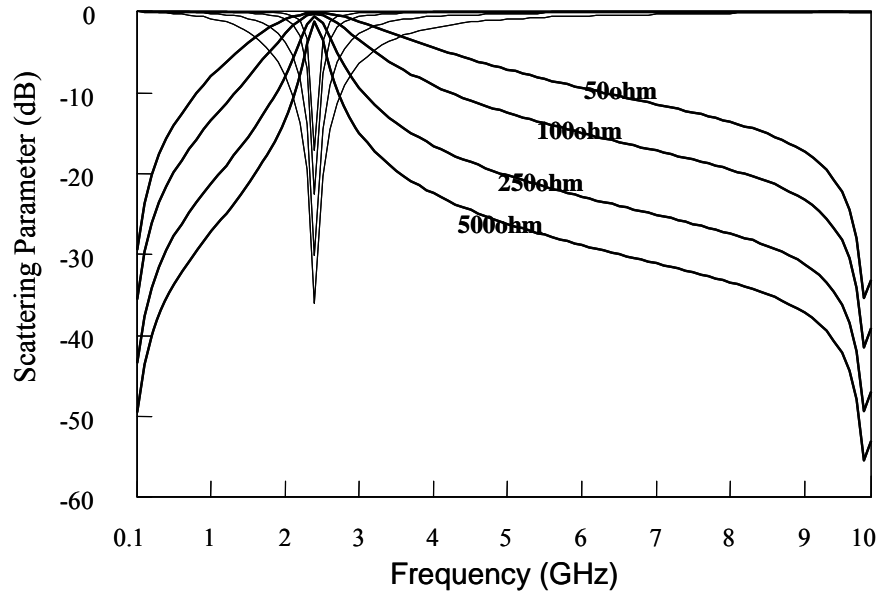
Fig. 2.6 Selectivity comparison with different load impedance

The circuitry in Fig. 2-7(a) is usually used to be the input stage of a high frequency amplifier. Assume that R, R_{in}, the resonant frequency, f_o, and the bandwidth, BW, are given, and L, C_1, and C_2 are the target to design. Additionally, the loss of L is so small to be ignored. Fig 2-7(a) is transformed into Fig 2-7(b) by applying serial-to-parallel transformation, and we can derive that C equals the series connection of C_1 and C_{se}.

Fig. 2.7 (a) The parallel to serial transformation of tapped capacitor (b) The serial to parallel transformation. (c) The ideally equivalent transformation

$$C = \frac{C_1 \times C_{se}}{C_1 + C_{se}} \tag{2-1}$$

In a high-Q circuitry with known f_o and BW, then Q_L can be derived as:

$$Q_L \cong \frac{f_o}{BW} \quad \text{or} \quad BW \cong \frac{f_o}{Q_L}. \tag{2-2}$$
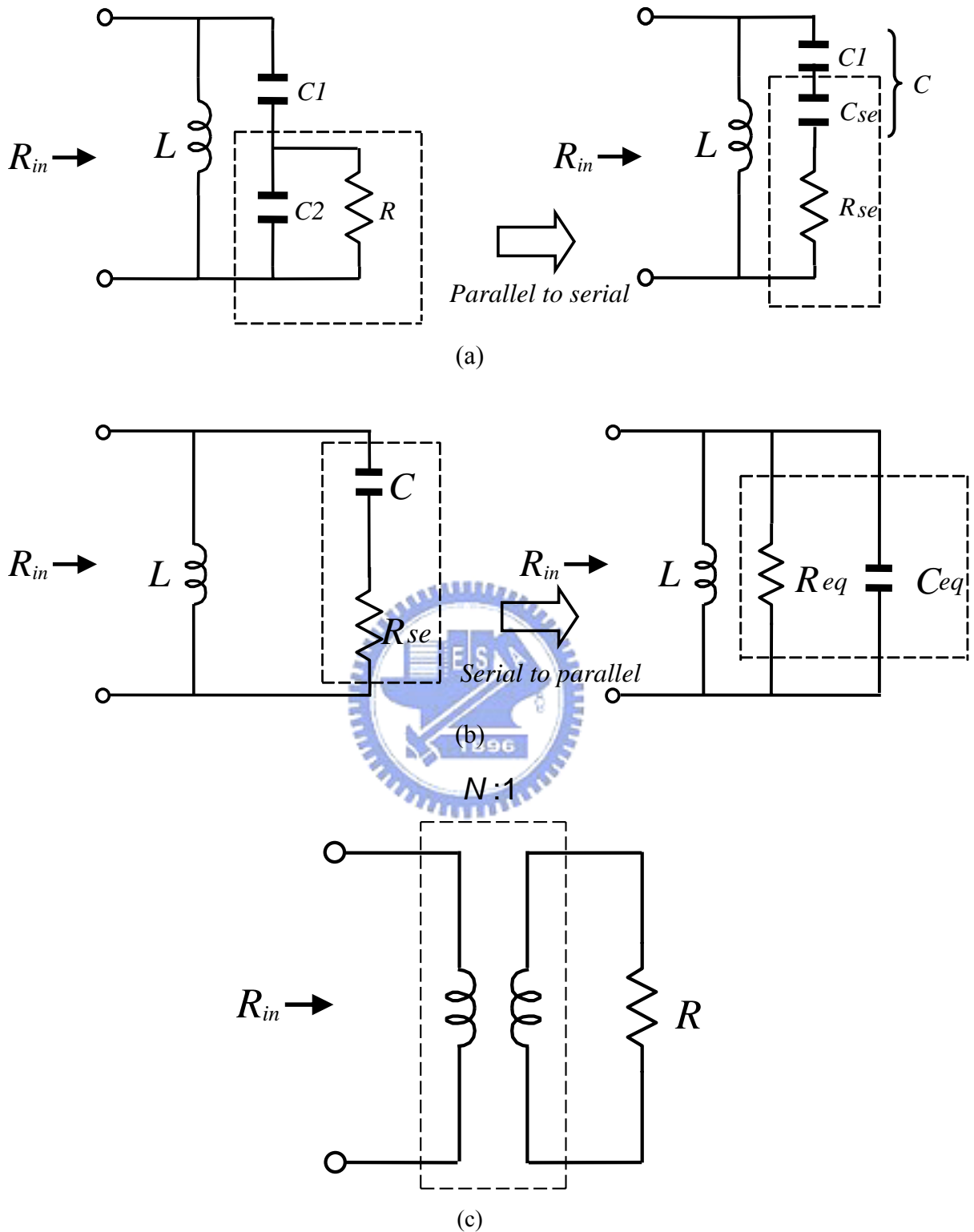
From parallel-to-serial impedance transformation, the relation between R_{in} and R_{se} is:

$$R_{se} = \frac{R_{in}}{Q_L^2 + 1} \tag{2-3}$$

(2-3) illustrates that R_{se} is derived from R_{in} and Q_L. Moreover, the Q-factor of parallel connection of C_2 and R is Q_P, by applying parallel-to-serial impedance transformation.

$$Q_P = \omega_o C_2 R \tag{2-4}$$

From parallel-to-serial impedance transformation, R_{se} can also be denoted as:

$$R_{se} = \frac{R}{1 + Q_P^2} \tag{2-5}$$

From (2-4), it is clearly that $Q_P \geqq 0$, thus R is no less than R_{se}. This explains that if a resistor is parallel-connected to an inductor or a capacitor, and the resultant resistor will always be smaller than the original resistor after parallel-to-serial impedance transformation. Because the right-hand side of (2-3) is equal to that of (2-5), Q_P can thus be derived as:

$$Q_P = \left(\left(Q_L^2 + 1 \right) \frac{R}{R_{in}} - 1 \right)^{1/2} \tag{2-6}$$

Moreover, at the resonant frequency, the characteristic of the circuitry impedance transformation is similar to an equivalent ideal transformer with ratio of turns, N, and

with ratio of impedance, N^2, as illustrated in Fig 2-7(c), assumed that

$$\frac{R_{in}}{R} = N^2 \tag{2-7}$$

By substituting (2-7) into (2-6),

$$Q_P = \left(\frac{\left(Q_L^2 + 1 \right)}{N^2} - 1 \right)^{1/2} \tag{2-8}$$

With $Q_L \geqq 10$, (2-8) can be simplified as:

$$Q_P = \left(\frac{Q_L^2}{N^2} - 1 \right)^{1/2} \tag{2-9}$$

If $Q_P > 10$, and assumed that $\dfrac{Q_L}{N} > 10$, (2-9) can be simplified again to:

$$Q_P \approx \frac{Q_L}{N} \tag{2-10}$$

(2-10) shows that approximation formula is applied if $Q_P > 10$, otherwise, non-approximation formula is used for $Q_P < 10$.

Design procedure for $Q_P < 10$

1. With known R, R_{in}, f_o, and BW, derive first that
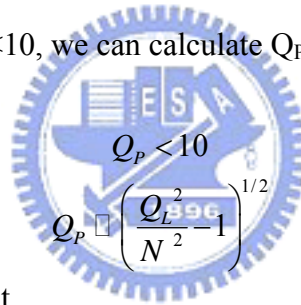
$$Q_L \cong \frac{f_o}{BW} \qquad (Q_L \geq 10)$$

$$C \cong \frac{1}{2\pi R_{in}(BW)}$$

$$L \cong \frac{1}{\omega_o^2 C}$$

$$\text{and} \quad N^2 = \left(\frac{R_{in}}{R}\right)$$

2. If $Q_P \cong \frac{Q_L}{N}$, shows that $Q_P < 10$, we can calculate Q_P from (2-9)

$$Q_P < 10$$

$$Q_P \cong \left(\frac{Q_L^2}{N^2} - 1\right)^{1/2}$$

3. Applying (2-4), we derive that

$$C_2 \cong \frac{Q_P}{\omega_o R}$$

Calculating that

$$C_{se} = \frac{C_2\left(1 + Q_P^2\right)}{Q_P^2}$$

4. Finally, calculate from (2-1) such that

$$C_1 = \frac{C_{se} \times C}{Q_{se} - C}$$

Design procedure for $Q_P > 10$
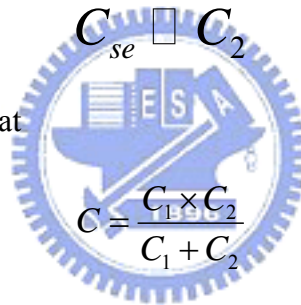
1. Q_L, C, L, and N can be derived from the counterpart of the previous procedure.

$$\frac{Q_L}{N} > 10$$

1. If $\frac{Q_L}{N} > 10$, calculate R_{se} and C_{se} by using approximation formula.

2. Given $C_2 \cong \frac{Q_P}{\omega_o R}$, and replace Q_P by $\frac{Q_L}{N}$, and assume $R_{in} \cong \frac{Q_L}{\omega_o C}$, thus we can

   get:

$$C_2 = NC$$

$$C_{se} \cong C_2$$

3. Therefore, we can derive that

$$C = \frac{C_1 \times C_2}{C_1 + C_2}$$

And substitute $C_2 = NC$ into the above equation, we find that

$$C_1 = \frac{N \times C}{N-1} = \frac{C_2}{N-1}$$

If substitute $C_2 = NC$ again into (2-7), it becomes that

$$\frac{R_{in}}{R} = N^2 = \left(\frac{C_2}{C}\right)^2 = \left(\frac{C_1 + C_2}{C_1}\right)^2 = \left(\frac{X_c}{X_{c2}}\right)^2$$

$$R_{in} = R\left(\frac{C_1 + C_2}{C_1}\right)^2 \tag{11}$$

Fig. 2.8 shows the circuit model of the design. The unbalanced to balanced band-pass filter is workable as demonstrated. To improve the selectivity performance, tapping skill is used to improve the circuit Q of resonator and to couple the signal to the next stage; the theory has been described on the previous section. This LTCC layout has two ground layers on Layer 1, Layer 31, which are connected for equal potential by side electrodes. These side electrodes should be connected with test instrument's ground through the evaluation board. Besides, it still has some problems that the number of LTCC layers must be increased to avoid the parasitic capacitance between the ground layer and the coupled transmission lines, which also means a higher fabrication cost.
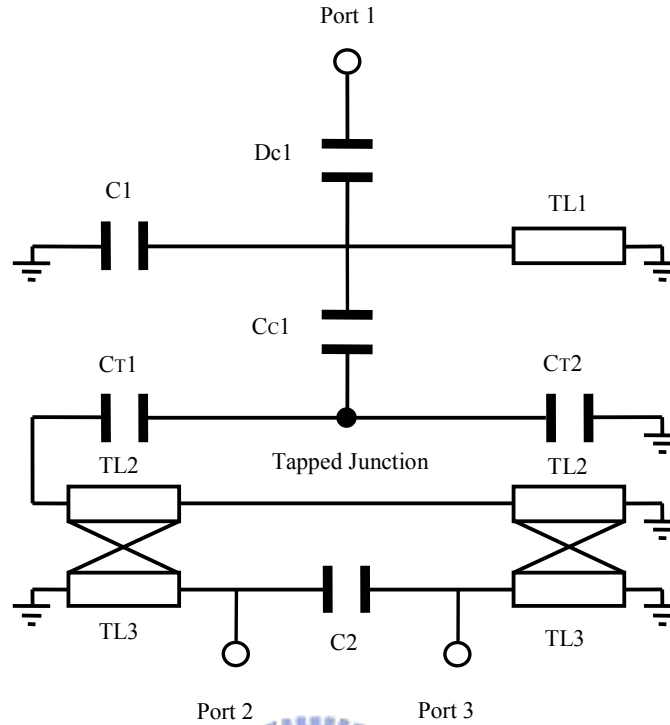
Fig. 2.8 The architecture of the unbalanced to balanced band-pass filter with tapped capacitor for selectivity improvement

The performance of the circuit simulation, a 2.4 GHz unbalanced to balanced band-pass filter is designed from this new structure. Fig. 2.9 shows the circuit simulation results. In this circuit design, the dielectric constant of LTCC substrate for each layer is 35 (at 2.5 GHz); the loss tangent is 0.002(at 2.5 GHz). The thickness of the metal plates (silver alloy) was 0.014 mm. The DC blocking capacitors Dc1, Cc1, are equal to 1.45 pF, 1.2 pF, respectively. The grounding capacitor C1 is equal to 3.0 pF. The tapped capacitor C_{T1}, C_{T2} are equal to 3.31 pF, 2.92 pF, respectively. The physical lengths of the transmission lines TL1 is equal to 1.58 mm, TL2 and TL3 are equal to 1.64mm, and their widths are equal to 0.15 mm. The spacing between each coupled

transmission line is equal to 0.6 mm. The input impedances of the three ports are equal

to 50 Ω, which means a 50 Ω unbalanced port and a 100 Ω balanced port. All the

resonators were merged to the same resonant frequency at 2.45 GHz. Therefore, the

magnitude response will have three poles in the pass band. According to the simulation

results in Fig.2.9, the magnitude imbalance between S21 and S31 is within 0.1dB in the

pass band, and the phase imbalance is very close to 0 degree from 1 GHz to 6 GHz. The

insertion loss and minimum return loss in the pass band are 4.0 dB and 20 dB
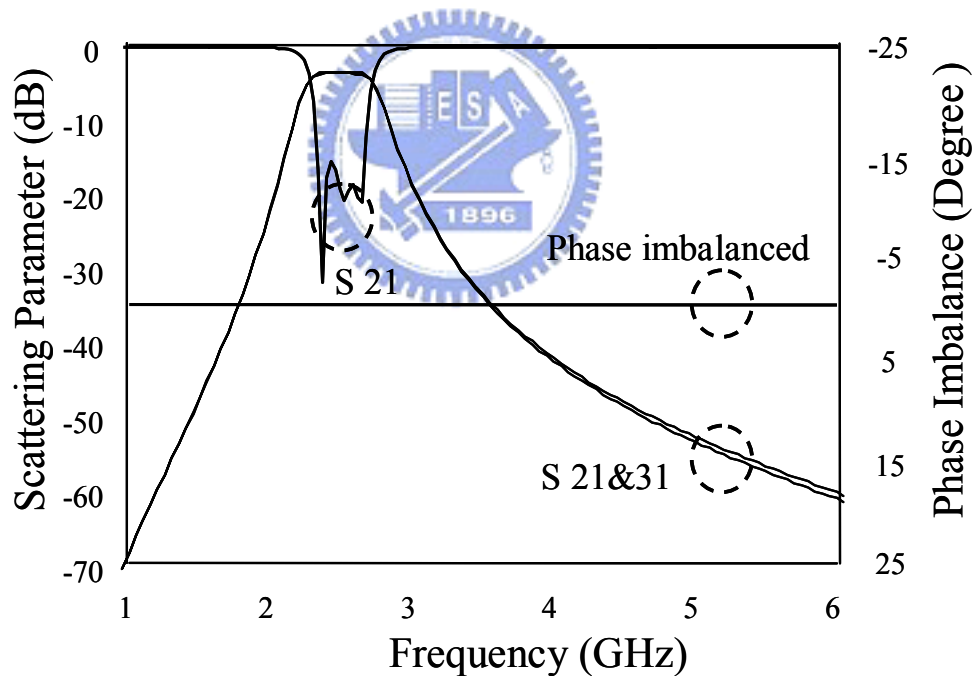
respectively.

Fig. 2.9 Scattering parameters and the phase imbalances of the proposed unbalanced to
balanced band-pass filter by circuit simulation

2.2 LTCC Layouts and EM Simulation

Based on the proposed filter schema, unbalanced to balanced band-pass filters with tapping junction for selectivity improvement were designed and fabricated using the LTCC process. In this circuit design, the dielectric constant of LTCC substrate for each layer is 35 (at 2.5 GHz); the loss tangent is 0.002(at 2.5 GHz). The thickness of the metal plates (silver alloy) was 0.014 mm. The structure of the proposed unbalanced to balanced band-pass filter is composed of the capacitors and the coupled transmission lines. The capacitors can be implemented in the LTCC substrate by metal-insulator-metal or interdigital-capacitor with the parallel plate capacitor formula of

$$C = \frac{\varepsilon A}{d} \tag{11}$$

where ε is the permittivity of the substrate, A is the overlapping area of the two plates, and d is the separated distance of the two plates. To cover the tolerance of fabrication, one of the plates should be larger than the other with at least 50 um in each side while designing a parallel plate capacitor. The physical size of the coupled transmission line depends on the circuit simulation result. However, it also needs fine tuning by EM simulation software. The component size is 2.5 mm × 2.0. mm × 1.0 mm and is designed using 31 layers of the LTCC substrate. The thickness of each layer is 0.031 mm. The designed component in this study which has a pass band centered at 2.45 GHz is typically applied in Bluetooth or IEEE 802.11 b/g WLAN. The first step is to adjust the filter's

component values with the circuit simulator to obtain the ideal frequency responses. Second, a multilayer LTCC structure is designed using the new component values, and simulated using the full-wave commercial package HFSS [14], which is a 3-D finite-element-based EM simulator. This LTCC layout has three ground layers on Layer 1, Layer 31 and small fraction on Layer 16, which are connected for equal potential by side electrodes. These side electrodes should be connected with test instrument's ground through the evaluation board. From Layer 2 to Layer11, Layer 17 to Layer22, and from Layer 26 to Layer 30, these are blank layers for diminishing parasitic capacitance. The capacitor Dc_1 which is connected to Port 1 (the input port) is generated by the metal plates on Layer 12, Layer13 and Layer 15 after equalizing the potentials on the metal plates of Layer 12 and Layer 15 by a via. The capacitor C_1 is formed by Layer 12 and Layer 15 which are coupled to the ground layer, Layer 1 and Layer 31, respectively. The capacitor C_2 which is connected to Port 2 and Port 3 (the output ports), respectively, is generated by the metal plates on Layer 23, Layer 24 and Layer 25. The capacitor C_{c1} which connects the first pole to the tapping junction of C_T1 and C_T2, respectively, is formed by the metal plates on Layer 12 and Layer 13. The capacitors C_{T1} and C_{T2} are cascaded to be the tapping junction, which are connected to the strip-lines TL_2 (on Layer13) and ground respectively, are generated by the metal plates on Layer 12, Layer 13, Layer 15, and Layer 16. The strip-lines TL_3 are located on Layer 23 with 0.15 mm width. Considering the limitation of minimum distance between two adjacent lines in fabrication, this coplanar layout can reduce the inaccuracy in LTCC fabrication. The required mutual inductance can be obtained using an appropriate coupling spacing. Significantly, the mutual inductance is formed by broadside-coupled with strip-lines TL_2

and TL_3. One end of the strip-line TL_1 is connected to Dc_1, C_1 and C_{c1} on Layer 13, and the other end is connected to ground by utilizing a via to connect the metal plates on Layer 13 and Layer 15 and join the grounded strip-line. Notably, the via contributes a small inductance to TL_1.
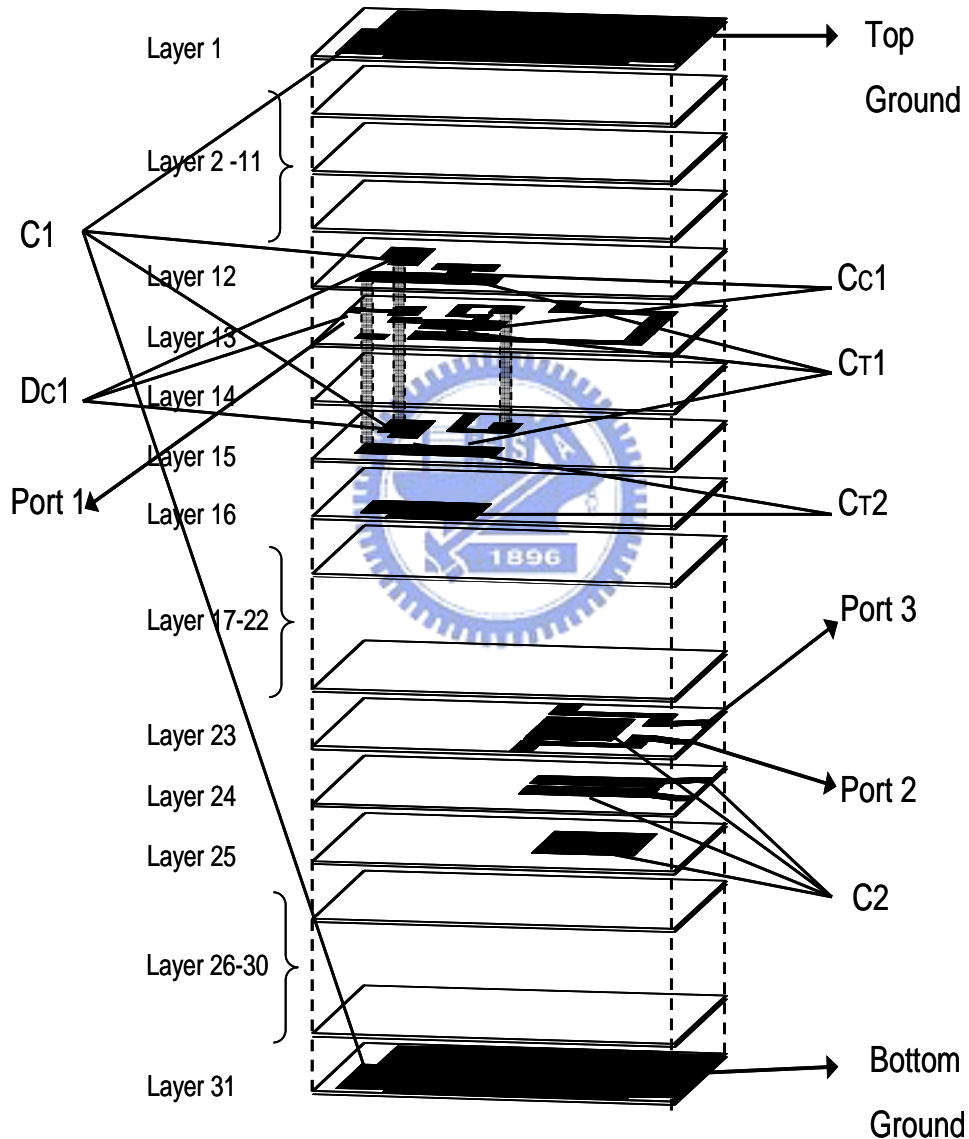

Fig. 2.10 Illustration of the 3D LTCC layout for EM simulation of a 2.4 GHz unbalanced to balanced band-pass filter with size of 2.5 mm × 2.0 mm ×1.0 mm

The ideal circuit simulation is calculated by the circuit simulator *Microwave Office* [13]; the EM simulation is simulated by the full-wave commercial package HFSS [14], which is a 3-D finite-element-based EM simulator. The results are presented in Fig. 2.11. The dash lines indicate the results of the EM simulation and the solid lines represent the ideal circuit simulation. Both simulation results match well as expectation. Due to the parasitic capacitance between Port 1 on Layer 13 and TL_3 on Layer 23, it produces a serial-LC resonator by parasitic capacitor and TL_3, thus causing a transmission zero near 5.3 GHz. In addition, the transmission zero located at 1.8GHz is also generated by a grounding serial-LC resonator, which is formed by the parasitic capacitor between Port 1 and the two sections of TL_2. These results demonstrate that the 3-D configuration is a good unbalanced to balanced band-pass filter with low in-band insertion loss and high out-of-band rejection around 45dB at 1.8/1.9 GHz and 25dB at the second harmonic frequency (4.9 GHz). In addition, the return loss approximates -18 dB. Fig. 2.11 also illustrates the EM simulation results of the LTCC layout.

(a)
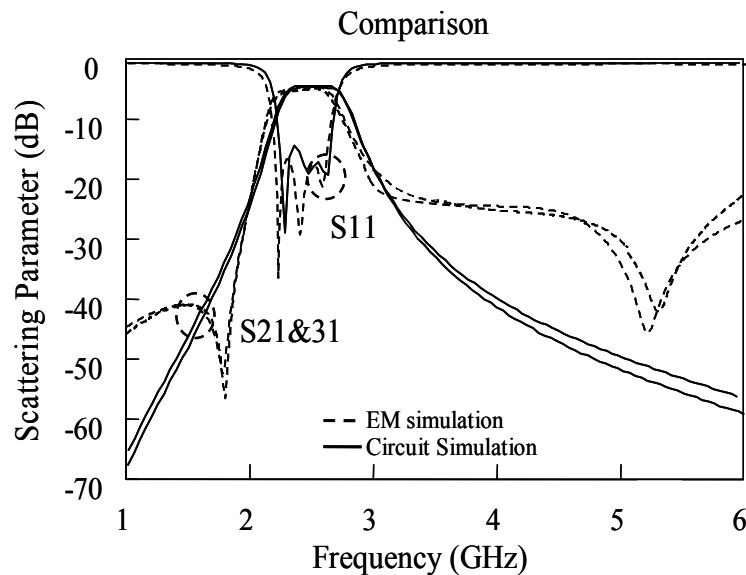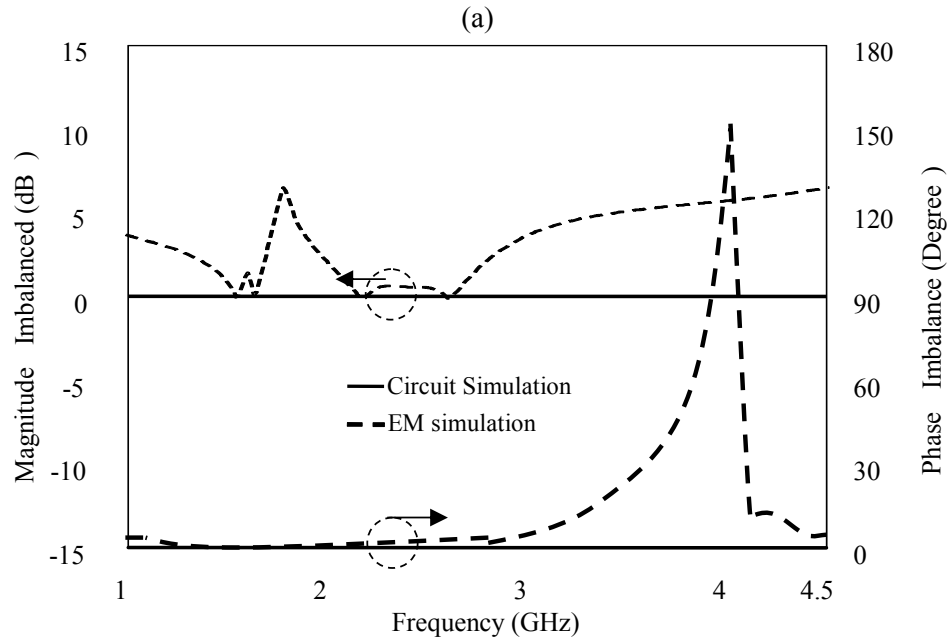
(b)

Fig. 2.11 Circuit simulation and EM simulation results: (a) Three-port scattering parameters and (b) Phase and magnitude imbalance responses

21
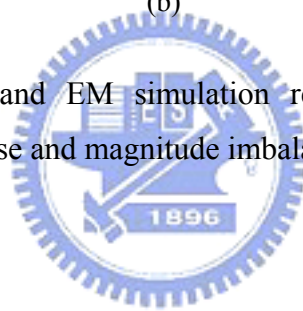
2.3 Experimental and measurement Results

After the analysis and EM simulation, the designed filter was fabricated using the LTCC process with dielectric constant of 35 (at 2.5 GHz), loss tangent of 0.004 (at 2.5 GHz) and thickness of the silver alloy of 0.017 mm. The commonly used printed-circuit board FR4 with dielectric constant of 4.4, loss tangent of 0.02, and thickness of 0.4 mm was applied as the test board to measure the performance of the fabricated LTCC filters. The measurement results are collected from Agilent ENA (E5071B) [15]-[16]. E5071B has four-port measurement capability, and it has the built-in functions to provide scattering parameters measurement in balanced mode and common mode without any external circuit or calculation, it is thus suitable for the measurement of the proposed unbalanced to balanced band-pass filter. Both the EM simulation and measurement results are shown and compared in Fig. 2.12(a), with EM simulation results in dashed line and measurement results in solid line. As shown in Fig. 2.12(a), the measured results agree with the simulations which have three transmission poles in the pass band. It can be observed from the S11 curves that the measurement result has a minimum return loss of 20 dB. It is a little regret for response that the poles were not obvious due to layout defectiveness, the insertion losses (S21 and S31) in the pass band at the two output ports are both less than 4.2 dB. Particularly, there is a transmission zero near 5.3 GHz as can be observed from both the EM simulation and measurement results. Significantly, the zero at the high-skirt side of the measured result is much deeper than that of the simulation. Fig. 2.12(b) shows the magnitude and phase imbalances of the unbalanced to balanced band-pass filter. According to the measured results, S21 and S31 have good balanced

performance in the pass band. Fig. 2.12(c) shows the details of the magnitude imbalances. As revealed from the measurement, the magnitude imbalanced is lower than 0.32 dB. Fig. 2.12(d) shows the details of the phase imbalances. The phase imbalance is smaller than 3 degrees in the pass band. After checking all the items, the measured response is found to agree well with the EM simulation. Fig. 2.13 shows the photograph of the fabricated LTCC unbalanced to balanced band-pass filter.
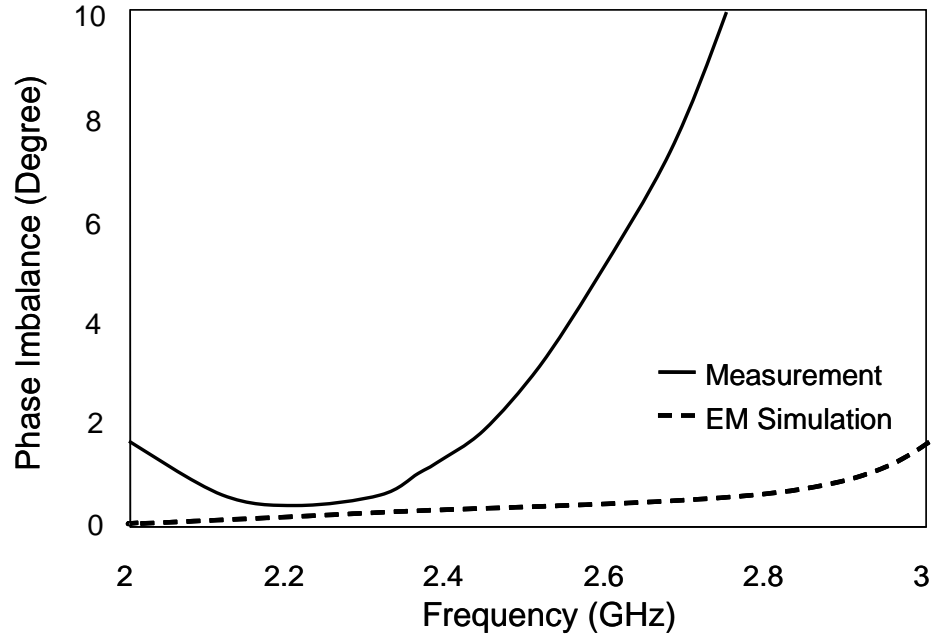

(a)

(b)

(c)

24
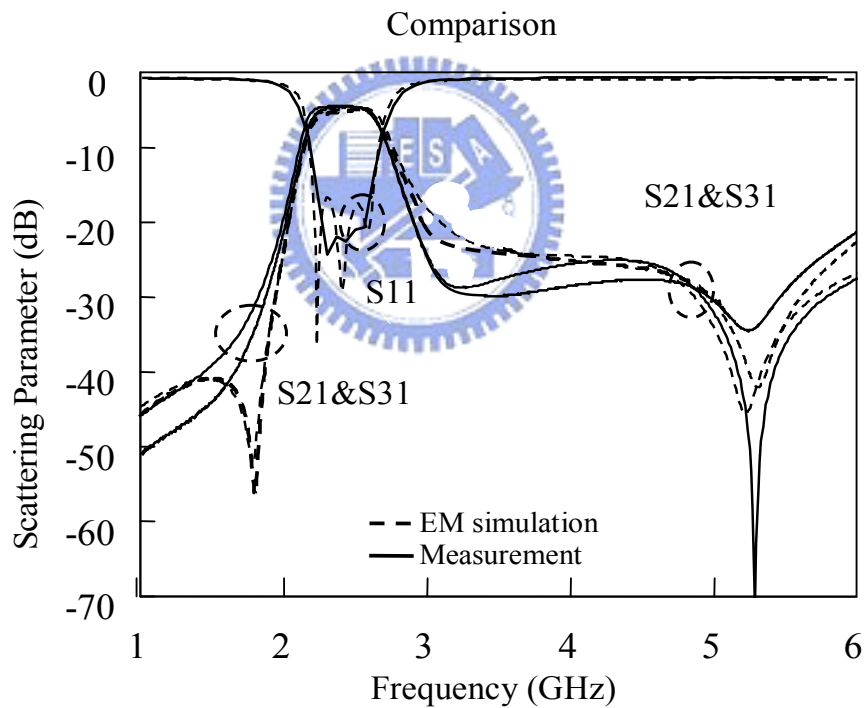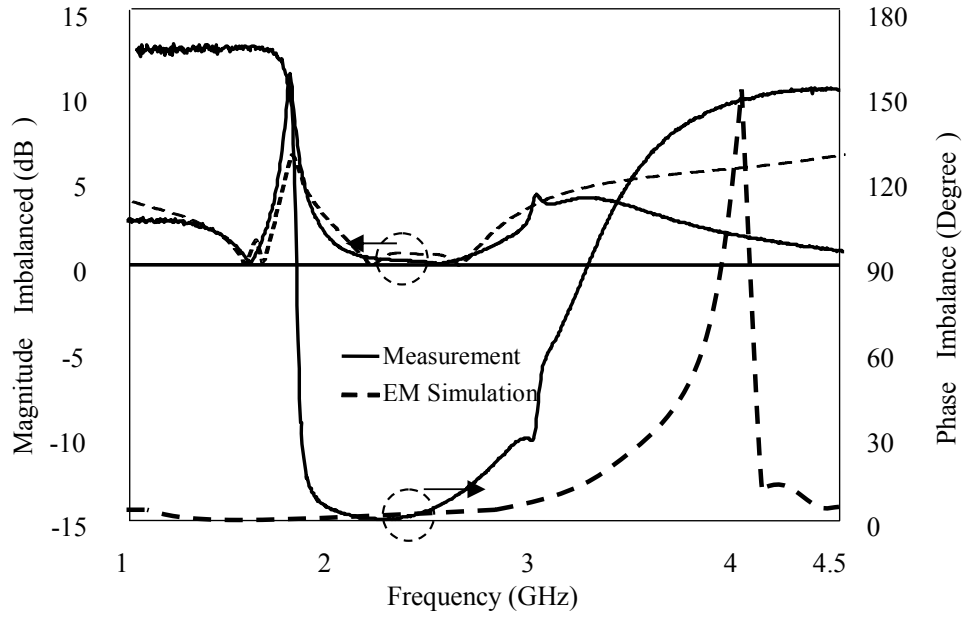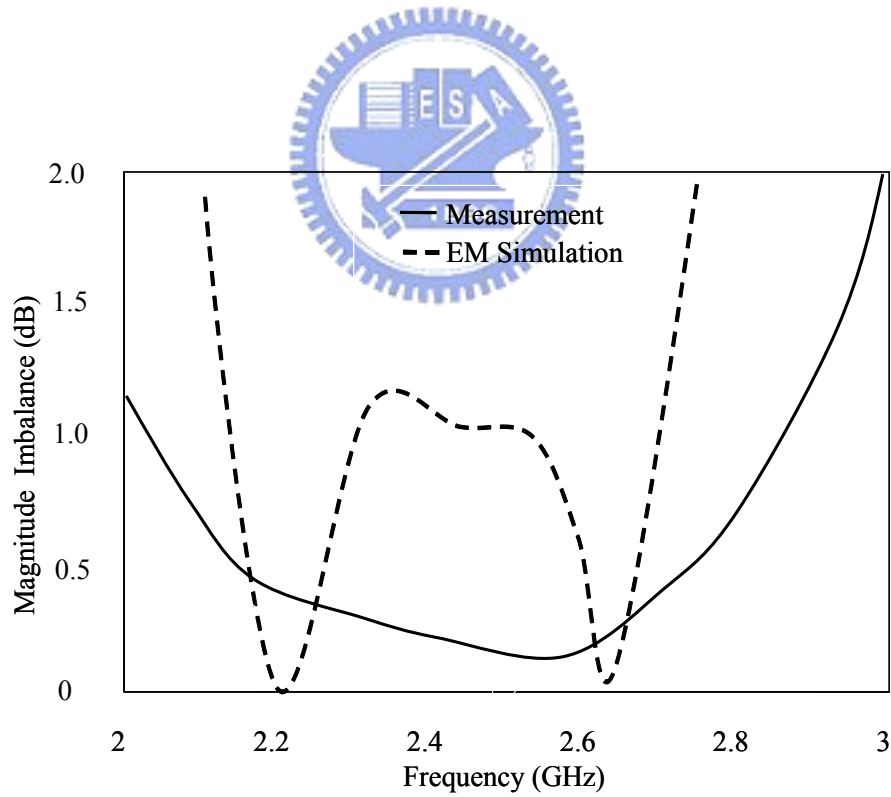
(d)

Fig. 2.12 Measurement and EM simulation results of the fabricated LTCC unbalanced to balanced band-pass filter. (a) Three-port scattering parameters, (b) Magnitude and phase imbalance characteristics, (c) The details of magnitude imbalance (d) The details of phase imbalance
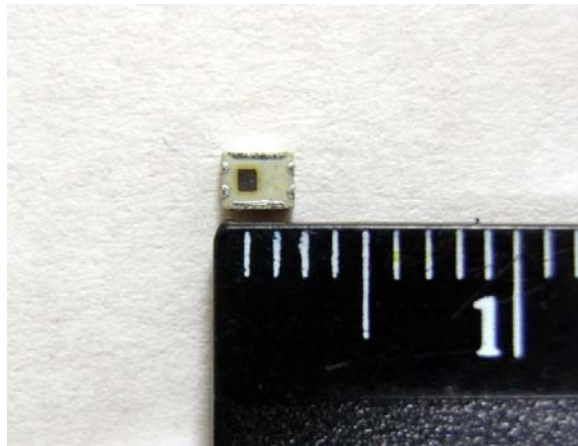

Fig. 2.13 Photograph of the LTCC balanced-to-unbalanced band-pass filter (size is 2.5 mm × 2.0 mm × 1.0 mm)

Chapter 3   Balanced to Balanced Band-pass Filter

In this chapter, it describes the modified lumped-distributed balun [10] for balanced to balanced filter applications, and detailed analysis of the structure and performance of the modified lumped-distributed balun is introduced. In order to verify the feasibility of the proposed structure, a 2.4 GHz balanced to balanced band-pass filter is designed by using circuit simulator *Microwave Office* [13]. RF balanced to balanced band-pass filter uses a resonator capacitor between the balanced output ports of Marchand balun. To verify the circuit simulation, we use low loss R/T Duroid/5880 as the substrate, and use the high Q discrete ceramic capacitor to implement the experiment circuit. The proposed balanced to balanced band-pass filter can use Low Temperature Co-fired Ceramic (LTCC) technology to meet the miniaturized size. The LTCC technology is successfully used for the component integration in RF section. There are two integration levels widely used in production: components integration and integration of components in the modules. Fig. 3.1 shows the application of the balanced to balanced band-pass filter between Dipole antenna and the RF frond-end stage. This is very attractive for balanced to balanced topology application.
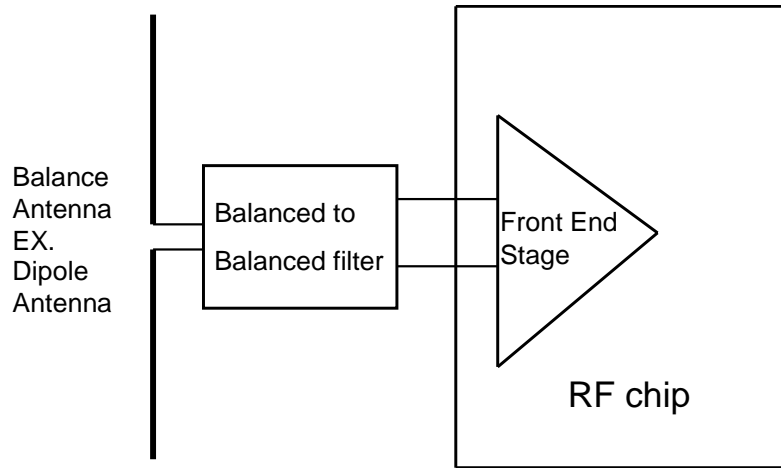
Fig.3.1.The application of Balanced to Balanced band-pass filter

The prototype of the balanced to balanced band-pass filter is based on the structure of Fig. 3.2(a) [10]-[12]. The capacitor C_2 is connected between the two balanced output ports of Marchand balun. Besides, one end of the transmission line TL2 is connected to ground. Thus, the capacitor and the two transmission lines can form a resonator. Therefore, we can derive a balance output port of the resonator. Then duplicating the same structure of the resonator using back-to-back method for signal coupling, as shown in Fig. 3.2(b), the prototype of the balanced to balanced band-pass filter is easily synthesized. The schema of Fig. 3.2 shows the structure migration of the balanced to balanced band-pass filter.
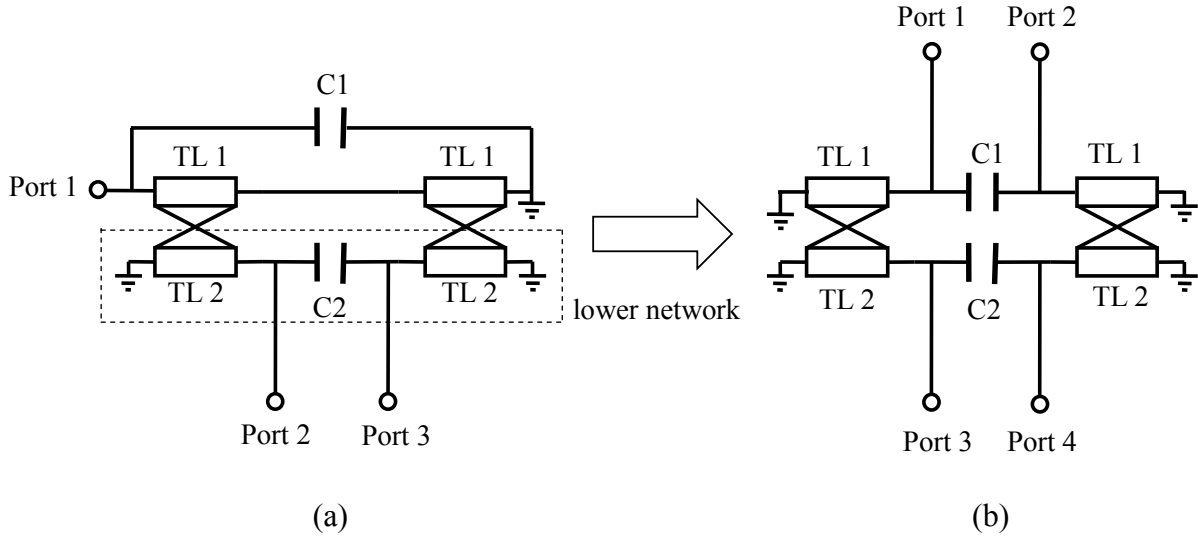
Fig. 3.2 Structure migration of the balanced to balanced band-pass filter

3.1 Circuit design of balanced to balanced band-pass filter

Fig. 3.3(a) shows the circuit simulation of 2.4 GHz balanced to balanced band-pass

filter which was calculated by the circuit simulator *Microwave Office* [4]. In this study,

the proposed filter was fabricated using the RT/Duroid 5880 as the substrate, which is

processed with dielectric constant of 2.20, thickness of 0.381mm, and thickness of the

copper of 0.008mm. All the discrete capacitors used for the circuit design are high Q

discrete capacitors made by Murata Co., Ltd, for improving the sharpness of the skirt

response. The DC blocking capacitors Dc1, Dc2, Dc3 and Dc4 are equal to 1.6 pF for

improving the return loss for each port. C_1 and C_2 are equal to 2.4 pF, which are located

between the balanced input and output portions of Marchand balun. Besides, one end of

each transmission line is connected to ground. As a result, two parallel-LC resonators

accompanied two poles can be generated, supporting the filter's pass band. The physical

lengths of the transmission lines TL1, TL2 are equal to 3.72 mm, and their widths are

equal to 2.0 mm. The spacing between each coupled transmission line is equal to 0.18 mm. The input impedances of the four ports are equal to 50 Ω. The resonators are merged to the same resonant frequency at 2.50 GHz. Therefore, the magnitude response will have two poles in the pass band. According to the circuit simulation results in Fig. 3.4, the phase imbalance is very close to 0 degree from 1 GHz to 6 GHz. In addition, the insertion loss and the minimum return loss in the pass band are 1.25 dB and 30 dB, respectively.
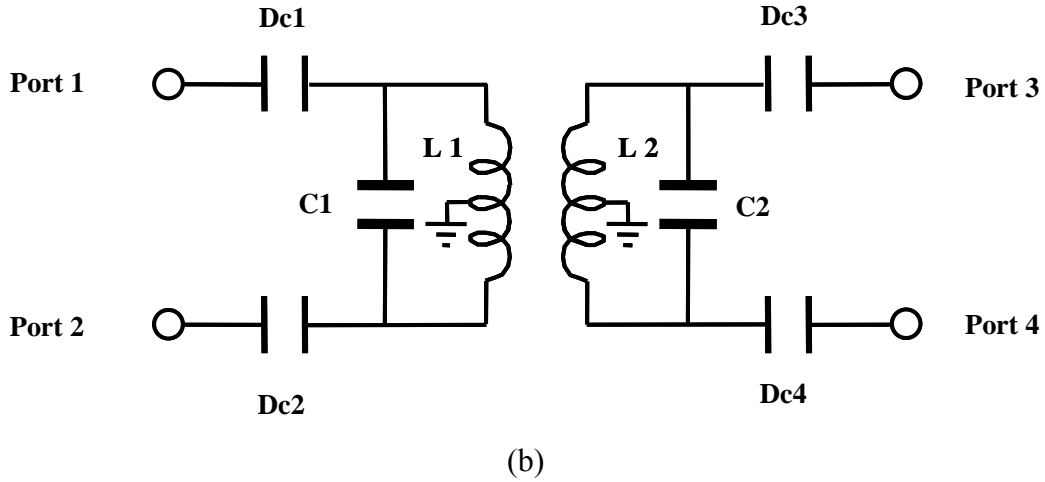

(a)

(b)
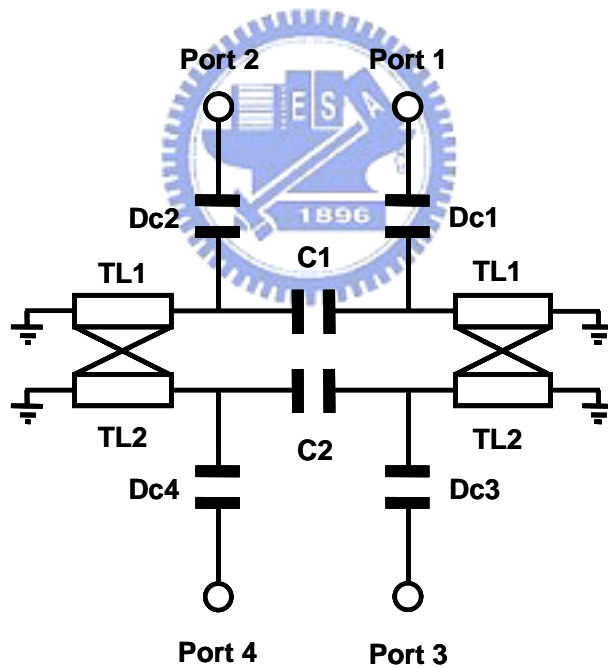
Fig. 3.3 (a) Schema of the proposed balanced to balanced band-pass filter (b) Equivalent
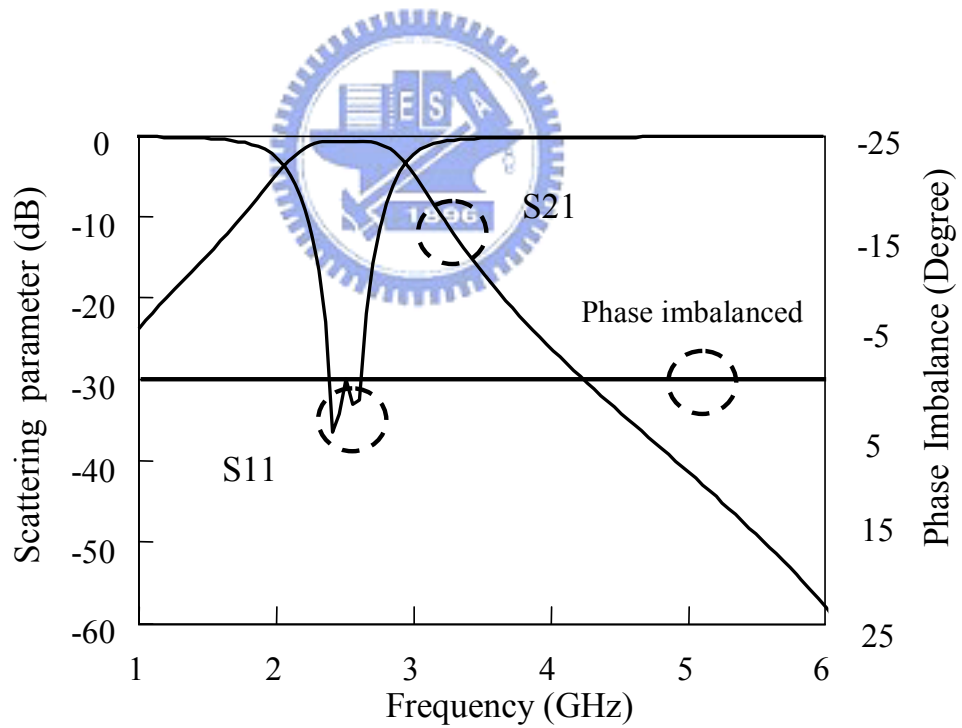   lumped-element circuit

Fig. 3.4 Scattering parameters (ideal responses) of the proposed balanced to balanced
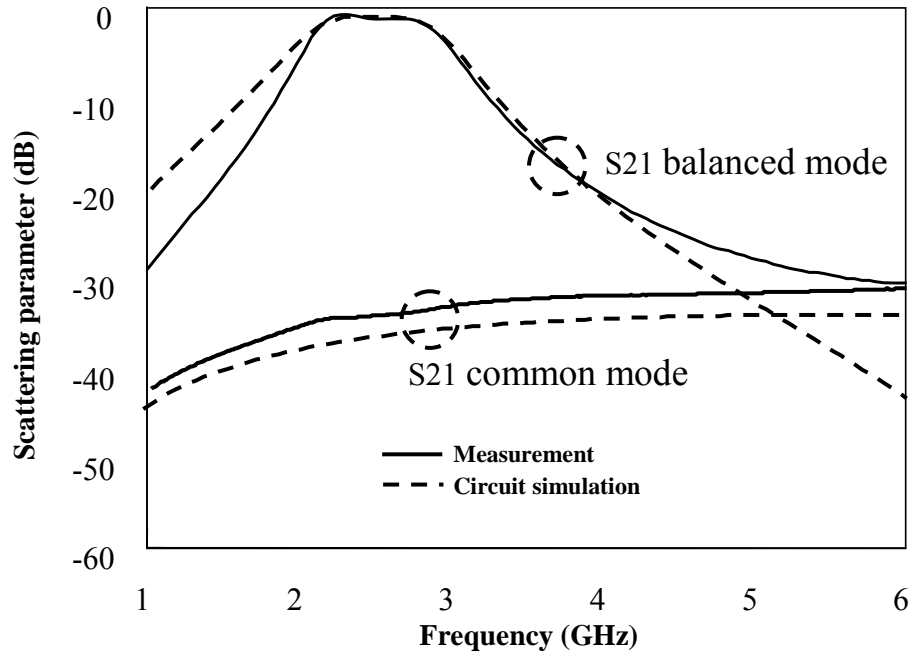   band-pass filter

3.2 Experimental and measurement Results

After the analysis and the circuit simulation, the proposed filters were fabricated using the RT/Duroid 5880 as the substrate, which is processed with dielectric constant of 2.20, thickness of 0.381mm, and thickness of the copper of 0.008mm. The measurement results are collected from Agilent ENA (E5071B) [15]-[16]. E5071B has four-port measurement capability, and it has the built-in functions to provide scattering parameters measurement in balanced mode and common mode without any external circuit or calculation. It is thus suitable for the measurement of the proposed balanced to balanced band-pass filter. For improving the response of the balanced to balanced band-pass filter, all the discrete capacitors used for the circuit design are the high Q discrete capacitor made by Murata Co., Ltd. Besides, two 1.2-pF capacitors with parallel connection are located on both the balanced input and balanced output ports in order to substitute the single 2.4-pF capacitor for reducing the parasitic inductance between terminals of the capacitor. Both the circuit simulation and measurement results were shown in Fig. 3.5, and were compared with circuit simulation results in dashed line and measurement results in solid line. Fig. 3.5(a) showed the measured scattering parameter was a little tilt, but it was still very close to the simulation result. Two transmission poles in the pass band can be observed from S11 curves of the measurement, with a minimum return loss of 20dB. The insertion losses (S21) in the pass band at the two output ports are both smaller than 1.25 dB. Fig. 3.5(b) shows the transmission performance of the balanced mode and the common mode. In the pass band, the maximum insertion loss of the balanced mode is 1.65 dB, and the minimum return loss of the common mode is 32 dB. Fig. 3.5(c) shows the detailed
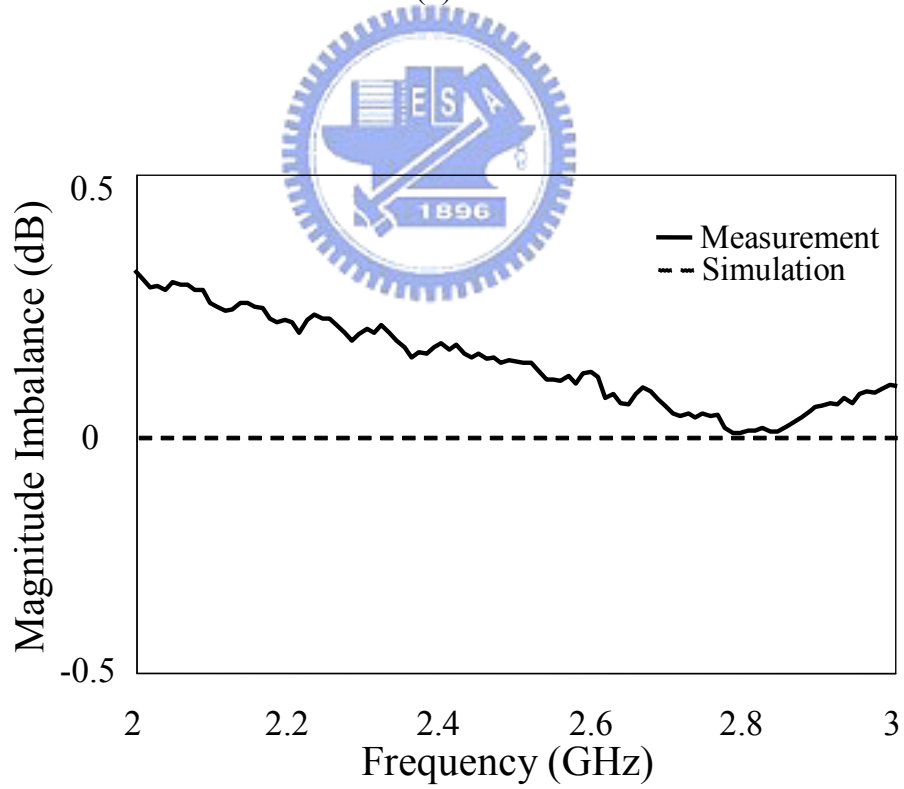
magnitude imbalances of the balanced to balanced band-pass filter. According to the measured results, port 3 and port 4 have good balanced performance in the pass band. From the measurement results, the magnitude imbalanced is lower than 0.2 dB. Fig. 3.5(d) shows the details of the phase imbalances. The measured response agrees well with that of the circuit simulation. The measurement result of the phase imbalance is smaller than 2.8 degrees in the pass band. Fig. 3.6 shows the photograph of the balanced to balanced band-pass filter using R/T Duroid/5880 with ε_r=2.2 and ¼ oz. (8 μm) electrodeposited copper foil. The board size is 40mm × 40mm × 0.38mm.
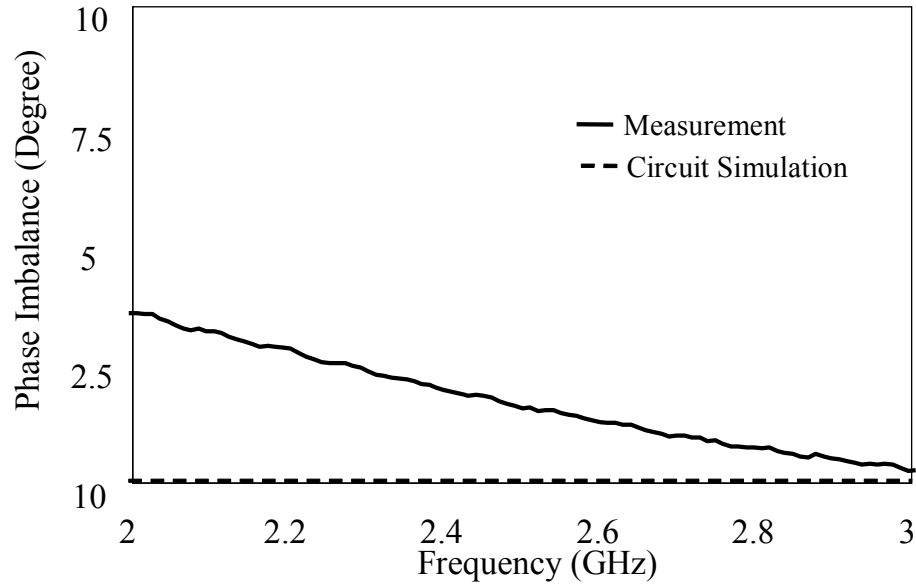

(a)

(b)

(c)

33
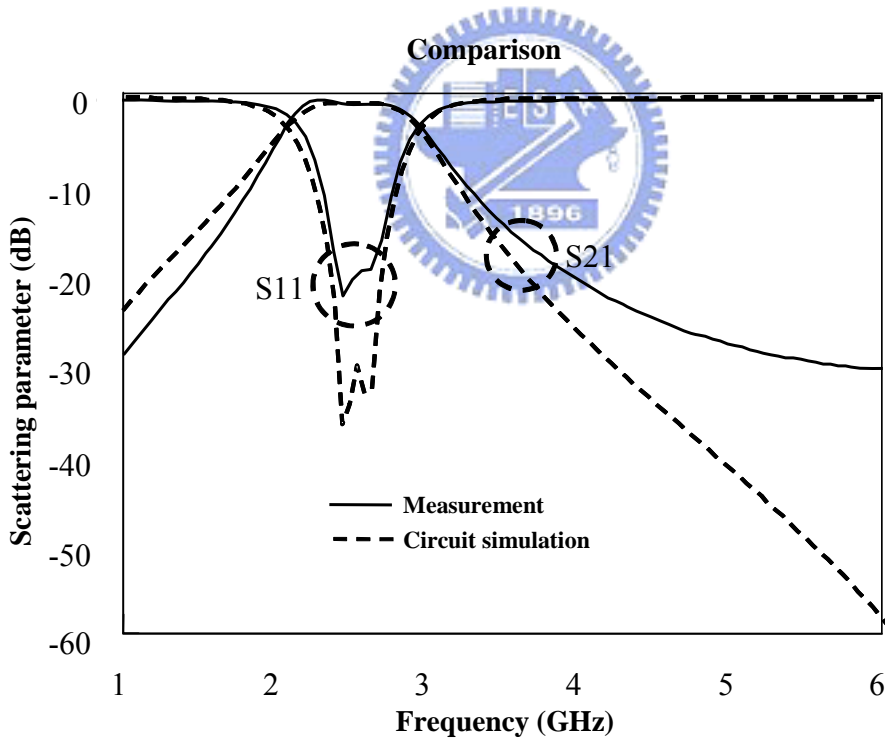
(d)

Fig. 3.5 Measurement and circuit simulation results of the fabricated balanced to balanced band-pass filter (a) Two port scattering parameters (b) balanced mode and common mode transmission characteristics (c) Magnitude imbalance characteristics (d) Phase imbalance characteristics
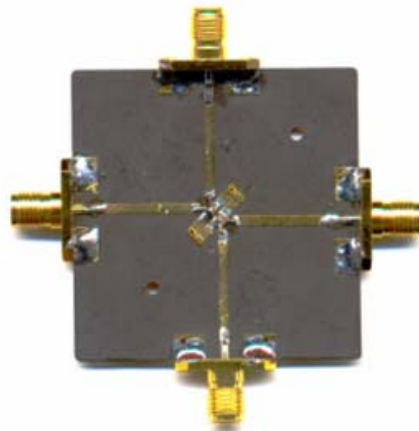

Fig. 3.6 Photograph of the balanced to balanced band-pass filter using R/T Duroid/5880, with ε_r=2.2 and ¼ oz. (8 μm) electrodeposited copper foil. The board size is 40mm ×4 0mm × 0.38mm.

Chapter 4　Conclusions

In this study, a lumped distributed balun as balanced band-pass filter has been proposed and operated in the 2.4 GHz – 2.5 GHz, and has been fabricated and measured to verify the design in a compact size using the LTCC technology. In the proposed configuration, the method of producing two resonators by using the two capacitors in distributed balun and the design concept of tapped-C configuration were clearly described in this study. The circuit design, LTCC layout, EM simulation and experimental results were thoroughly described. Although some parasitic capacitance produced between the coupled transmission lines generated transmission zeros at 1.8GHz and 5.3GHz, the responses are not affected much. The measurement results were found to agree well with the EM simulation results. The fabricated unbalanced to balanced band-pass filter was compact with low insertion loss in the pass-band and high suppression in the rejection area. This design can be applied in Bluetooth or IEEE 802.11b/g WLAN (Wireless Local Area Network).

Furthermore, a RF balanced to balanced band-pass filter based on modification of the common Marchand balun is proposed. The circuit simulation and experimental results were thoroughly described. The measured S-parameters show excellent agreement with the circuit simulation results. To verify the circuit simulation, we use low loss R/T Duroid/5880 substrate and high Q discrete ceramic capacitor to implement the experiment circuit. The measurement results were found to agree well with the circuit simulations. The proposed balanced to balanced band-pass filter operating at the 2.4GHz–2.5GHz can also be applied in Bluetooth or IEEE 802.11b/g WLAN (Wireless Local Area Network).

References

[1] B. Razavi, *Design of Analog CMOS Integrated Circuit*. Boston, MA: McGraw-Hill, 2001.

[2] K.-T. Chen and S.-J. Chung, "A Novel Compact Balanced-to-Unbalanced Low-Temperature Co-Fire Ceramic Bandpass Filter with Three Coupled Lines Configuration," *IEEE Trans. Microwave Theory Tech.*, vol. 56, no. 7, pp. 1714–1720, Jul. 2008.

[3] C. M. Tsai, and K. C. Gupta, "CAD procedures for planar re-entrant type couplers and three-line baluns," in *IEEE MTT-S Int. Microwave Symp. Dig.*, 1993, pp. 1013-1016.

[4] C. Cho, and K. C. Gupta, "A new design procedure for single-layer and two-layer three-line baluns," *IEEE Trans. Microwave. Theory Tech.*, vol. 46, no. 12, pp. 2514–2519, Dec. 1998.

[5] B. H. Lee, D. S. Prak, S. S. Park, and M. C. Park, "Design of new three-line balun and its implementation using multilayer configuration," *IEEE Trans. Microwave. Theory Tech.*, vol. 54, no. 4, pp. 1405–1414, June 2006.

[6] L. K. Yeung and K. L. Wu, "A compact second-order LTCC bandpass filter with two finite transmission zeros," *IEEE Trans. Microwave Theory Tech.*, vol. 51, pp. 337-341, February 2003.

[7] Ching-Wen Tang, Yin-Ching Lin, and Chi-Yang Chang, "Realization of Transmission Zeros in Combline Filters Using an Auxiliary Inductively Coupled Ground Plane," in *IEEE Trans. Microwave Theory Tech.*, vol. 51, pp. 2112-2118, Oct. 2003.

[8] C. F. Chang and S. J. Chung, "Bandpass filter of serial configuration with two finite transmission zeros using LTCC technology," *IEEE Trans. Microwave Theory Tech.*, vol. 53, pp. 2383-2388, July 2005.

[9] Y.-S. Lin, C.-H. Wang, C. H. Wu, and C. H. Chen, "Novel compact parallel-coupled microstrip bandpass filters with lumped-element K-inverters," *IEEE Trans. Microwave Theory Tech.*, vol. 53, no. 7, pp.2324–2328, Jul. 2005.

[10] R. Kravchenko, K. Markov, D. Orlenko, G. Sevskiy, and P. Heide, "Implementation of a miniaturized lumped-distributed balun in balanced filtering for wireless applications," in *Proc. Eur. Microwave Conf.*, 2005, pp. 1303–1306.

[11] Kian Sen Ang, Yoke Choy Leong, Chee How Lee, *"Analysis and Design of Miniaturized Lumped-Distributed Impedance-Transforming Baluns,"* IEEE, Transactions on microwave theory and techniques, Vol. 51, No. 3, 2003.

[12] N. Marchand, *"Transmission line conversion transformers,"* Electronics, vol. 17, No. 12, pp. 142-145, Dec. 1942.

[13] *Microwave Office*, Applied Wave Research, Inc., El Segundo, CA, 2002.

[14] *HFSS*, Ansoft Corporation, Pittsburgh, PA.

[15] *"Agilent E5070B/E5071B ENA Series RF Network Analyzers User's Guide,"* 2nd ed. Agilent Technol., CA, 2003..

[16] Product Note 8510-8A, Agilent Network Analysis Applying the 8510 TRL Calibration for Non-Coaxial Measurements.